

A SHM method for identifying damage based on VARX modelling and substructuring approach

Unai UGALDE¹, Javier ANDUAGA¹, Fernando MARTÍNEZ², Aitzol ITURROSPE³

¹Dpt Control and Monitoring, IK4-Ikerlan Technology Research Centre, Mondragon, Spain (uugalde@ikerlan.es)

²Dpt Microsystems, IK4-Ikerlan Technology Research Centre, Mondragon, Spain

³Dpt Electronics and Computer Sciences, Mondragon Goi Eskola Politeknikoa, Mondragon, Spain

Abstract

A novel SHM method is proposed for damage localisation and quantification combining the substructuring approach and Vector Auto-Regressive with Exogenous input (VARX) models. The substructuring approach aims to divide the monitored structure into several isolated substructures. Each individual substructure is modelled as a VARX model, and the health of each substructure is determined analysing the variation of the VARX model's *coefficients*. The method allows determining whether the isolated substructure is damaged, and besides allows locating and quantifying the damage within the substructure. It is not necessary to have a physics-based model of the structure and only vibration data of the substructures are required to estimate their VARX models. The proposed method is validated by simulations and experimentally in a five-story structure.

Keywords: Substructuring, Structural Health Monitoring, Damage identification, VARX modelling

1. INTRODUCTION

Structural Health Monitoring (SHM) is a technological area which develops a damage detection and characterization strategies for engineering structures [1]. SHM is regarded as a very important engineering field in order to secure structural and operational safety; issuing early warnings on damage or deterioration, avoiding costly repairs or even catastrophic failures [2].

Most of the existing vibration based SHM methods can be classified into two different approaches: global approaches and local approaches [3]. In the global approaches, the goal is to monitor the health of the entire structure. These global methods have been tested and implemented in different types of structures during the last 30-40 years [4]. However, for many large systems, global monitoring is not viable due to the lack of sensitivity of global features to local damages, inaccuracies of developed models etc[5]. On the other hand, local SHM methods are focused on evaluating the condition of smaller parts within the entire structures by means of substructuring approach. This approach aims to overcome global method's limitations, dividing the whole structure into substructures and analysing each one individually.



Several papers have been published proposing substructuring methods for large scale structures. Koh et al [6] presented a “divide and conquer” strategy to monitor large structures based on the division of the whole structure into isolated substructures. For each substructure, structural parameters are identified using the extended Kalman filter (EKF). However, the EKF usually requires a physics-based model, which is not always available [7]. Most recently, Xing et al [8] and Lei et al [9] proposed another substructural damage detection method using Auto-Regressive Moving Average with eXogenous input (ARMAX) models. The substructures are represented by an ARMAX model and the natural frequency of each substructure is extracted from the mentioned model for its posterior analysis. Nonetheless it is preferably applicable to small and simple structures.

The authors of this article proposed in [10][11] a damage localisation and quantification method based on substructuring approach and Vector Auto-Regressive with eXogenous input (VARX) models. The proposed method was able to monitor multi-DOF substructures analysing the variation of the VARX models. Only vibration data was measured from the substructures and it was not necessary to have a physics-based model of the structure. This new article incorporates some improvements over the initial method and an experimental validation in a five-story structure.

The rest of the paper is organised as follows. In section 2, the proposed method is presented. In section 3, the method is evaluated by series of simulations. In section 4, the method is validated in a five-story structure. Finally the concluding remarks are presented in section 5.

2. THE PROPOSED METHOD

The dynamics of the structure is described by a lumped parameter model. It is assumed that the structure consists of bars and the forces can only be transmitted along the axial direction of these bars. Besides, the structure is subjected to arbitrary external loading that is assumed to be known and could act on any node.

The structure is divided into different isolated substructures. The substructures have n internal (i) and m interface (j) nodes. The interface nodes are located in the border between the selected substructure and the remaining structure. The internal nodes are located within the substructure and they are not connected to the nodes of the remaining structure.

The dynamic equation for an internal node l is formulated as follows:

$$M_{il}\ddot{\mathbf{z}}_{il} = \sum_{p=1}^N (f_p(\mathbf{z}_i, \dot{\mathbf{z}}_i, \mathbf{z}_j, \dot{\mathbf{z}}_j)) + \mathbf{f}_{il} \quad (1)$$

where M_{il} is the lumped mass matrix of the internal node l and $\ddot{\mathbf{z}}_{il}$ is a vector that contains the accelerations of the internal node l in x , y and z axes respectively (\ddot{z}_{ilx} , \ddot{z}_{ily} and \ddot{z}_{ilz}). \mathbf{f}_p is a vector with linear or non-linear functions used to calculate the total force applied in the internal node l by the N nodes connected to him. $\mathbf{z}_i, \dot{\mathbf{z}}_i, \mathbf{z}_j$ and $\dot{\mathbf{z}}_j$ are the displacement and velocity vectors of the internal and interface nodes that are connected to the internal node l in x , y and z axes. Furthermore, \mathbf{f}_{il} contains the external force applied in the internal node l in x , y and z axes (f_{ilx} , f_{ily} , f_{ilz}).

Expanding \mathbf{f}_p function as Taylor series [12] and selecting only the first term, the dynamic equations for an internal node l are stated as:

(2)

$$\begin{aligned}
m_{i1x} \ddot{z}_{i1x} &= \sum_{p=1}^N (k_{i1x-px} (z_{i1x} - z_{px}) + k_{i1x-py} (z_{i1y} - z_{py}) + k_{i1x-pz} (z_{i1z} - z_{pz}) + c_{i1x-px} (\dot{z}_{i1x} - \dot{z}_{px}) + c_{i1x-py} (\dot{z}_{i1y} - \dot{z}_{py}) + c_{i1x-pz} (\dot{z}_{i1z} - \dot{z}_{pz})) + f_{i1x} \\
m_{i1y} \ddot{z}_{i1y} &= \sum_{p=1}^N (k_{i1y-px} (z_{i1x} - z_{px}) + k_{i1y-py} (z_{i1y} - z_{py}) + k_{i1y-pz} (z_{i1z} - z_{pz}) + c_{i1y-px} (\dot{z}_{i1x} - \dot{z}_{px}) + c_{i1y-py} (\dot{z}_{i1y} - \dot{z}_{py}) + c_{i1y-pz} (\dot{z}_{i1z} - \dot{z}_{pz})) + f_{i1y} \\
m_{i1z} \ddot{z}_{i1z} &= \sum_{p=1}^N (k_{i1z-px} (z_{i1x} - z_{px}) + k_{i1z-py} (z_{i1y} - z_{py}) + k_{i1z-pz} (z_{i1z} - z_{pz}) + c_{i1z-px} (\dot{z}_{i1x} - \dot{z}_{px}) + c_{i1z-py} (\dot{z}_{i1y} - \dot{z}_{py}) + c_{i1z-pz} (\dot{z}_{i1z} - \dot{z}_{pz})) + f_{i1z}
\end{aligned}$$

where z_{i1x} , z_{i1y} , z_{i1z} and \dot{z}_{i1x} , \dot{z}_{i1y} , \dot{z}_{i1z} are the displacements and velocities of the internal node 1 and z_{px} , z_{py} , z_{pz} and \dot{z}_{px} , \dot{z}_{py} , \dot{z}_{pz} are the displacements and velocities of the N (internal or interface) nodes that are connected to the internal node 1. Furthermore, k and c are coefficients related to the stiffness and damping values of the N bars that are connected to the internal node 1.

The n internal nodes of the substructure are represented as in equation 1-2 in order to obtain the substructural dynamic equation. The finite central difference method [13] is used to obtain an approximation of the displacements from the velocity and acceleration data. The substructural dynamic equation in matrix form and in terms of displacements is represented as follows:

$$\begin{aligned}
\begin{bmatrix} z_{i1x}(n) \\ z_{i1y}(n) \\ z_{i1z}(n) \\ \dots \\ z_{inx}(n) \\ z_{iny}(n) \\ z_{inz}(n) \end{bmatrix} &= -A_1 \begin{bmatrix} z_{i1x}(n-1) \\ z_{i1y}(n-1) \\ z_{i1z}(n-1) \\ \dots \\ z_{inx}(n-1) \\ z_{iny}(n-1) \\ z_{inz}(n-1) \end{bmatrix} - A_2 \begin{bmatrix} z_{i1x}(n-2) \\ z_{i1y}(n-2) \\ z_{i1z}(n-2) \\ \dots \\ z_{inx}(n-2) \\ z_{iny}(n-2) \\ z_{inz}(n-2) \end{bmatrix} \\
&+ B_{10} \begin{bmatrix} z_{j1x}(n) \\ z_{j1y}(n) \\ z_{j1z}(n) \\ \dots \\ z_{jmx}(n) \\ z_{jmy}(n) \\ z_{jnz}(n) \end{bmatrix} + B_{11} \begin{bmatrix} z_{j1x}(n-1) \\ z_{j1y}(n-1) \\ z_{j1z}(n-1) \\ \dots \\ z_{jmx}(n-1) \\ z_{jmy}(n-1) \\ z_{jnz}(n-1) \end{bmatrix} + B_{12} \begin{bmatrix} z_{j1x}(n-2) \\ z_{j1y}(n-2) \\ z_{j1z}(n-2) \\ \dots \\ z_{jmx}(n-2) \\ z_{jmy}(n-2) \\ z_{jnz}(n-2) \end{bmatrix} + B_{21} \begin{bmatrix} F_{i1x}(n-1) \\ F_{i1y}(n-1) \\ F_{i1z}(n-1) \\ \dots \\ F_{inx}(n-1) \\ F_{iny}(n-1) \\ F_{inz}(n-1) \end{bmatrix}
\end{aligned} \tag{3}$$

where z_{i1x} , ..., z_{inz} are the displacements of the n internal nodes and z_{j1x} , ..., z_{jnz} are the displacements of the m interface nodes.

Equation (3) could be regarded as a VARX model [14], where z_{i1x} , ..., z_{inz} correspond to the endogenous variables and z_{j1x} , ..., z_{jnz} and F_{i1x} , ..., F_{imz} correspond to the exogenous variables. A_1 and A_2 are the endogenous coefficient matrices and B_{10} , B_{11} , B_{12} , and B_{21} are the exogenous coefficient matrices. The elements of the mentioned matrices are related to the physical properties of the substructure.

In the proposed method, the displacements in the internal and interface nodes of the substructure are measured and the corresponding VARX model is estimated. It is assumed that the substructure is healthy at the beginning, so the VARX model estimated with the initial data is taken as a reference. Displacement data is measured again when the substructure must be evaluated and the corresponding VARX model is estimated. In the proposed method, endogenous and exogenous coefficient matrices of these new VARX models are compared to the same matrices of the reference model and as a result the condition of the substructure is evaluated.

3. EVALUATION BY SIMULATIONS

A five-story building's finite element model has been developed. Each floor has one steel slab, which is $200 \times 200 \times 10 \text{ mm}^3$ and four vertical and two diagonal steel plates, which are $160 \times 30 \times 2 \text{ mm}^3$ and $203 \times 30 \times 2 \text{ mm}^3$ respectively. The first five natural frequencies of the model are 7.36 Hz, 20.29 Hz, 31.56 Hz, 42.53 Hz and 51.59 Hz.

As it is shown in figure 1, a substructure formed by three floors is selected for its monitoring. Horizontal accelerations and displacements \ddot{z}_{3x} , z_{3x} , \ddot{z}_{4x} , z_{4x} , \ddot{z}_{5x} and z_{5x} correspond to internal DOFs, whereas \ddot{z}_{2x} and z_{2x} correspond to interface DOFs. The structure is excited applying a Gaussian white noise force out of the substructure.

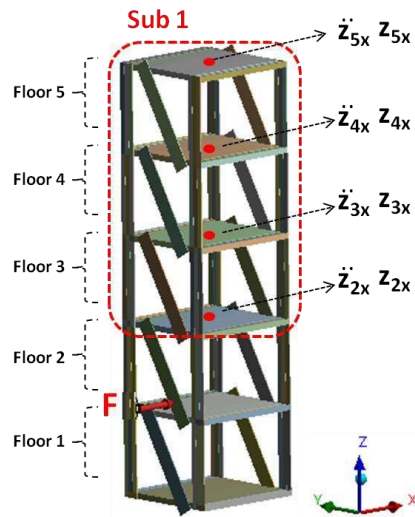


Figure 1: Five-story building's model

The dynamic equations for the isolated substructure could be formulated as:

$$\begin{aligned}
 m_3 \ddot{z}_{3x}(t) &= -k_3(z_{3x}(t) - z_{2x}(t)) - k_4(z_{3x}(t) - z_{4x}(t)) \\
 m_4 \ddot{z}_{4x}(t) &= -k_4(z_{4x}(t) - z_{3x}(t)) - k_5(z_{4x}(t) - z_{5x}(t)) \\
 m_5 \ddot{z}_{5x}(t) &= -k_5(z_{5x}(t) - z_{4x}(t))
 \end{aligned} \tag{4}$$

where m_3 , m_4 and m_5 and k_3 , k_4 and k_5 represent the substructural floor's mass and stiffness values.

Following the procedure described in section 2, the dynamical behaviour of the substructure can be described by a VARX model stated in equation 5. The endogenous variables are the measured horizontal displacements in floors 3 (z_{3x}), 4 (z_{4x}) and 5 (z_{5x}), whereas the exogenous variable is the

measured horizontal displacement in floor 2 (z_{2x}). Equation (5) shows that the matrices A_1 and B_1 depend on the substructural parameters $m_3, m_4, m_5, k_3, k_4, k_5$, as well as the sampling period (T_s).

$$\begin{aligned} \begin{bmatrix} z_{3x}(n) \\ z_{4x}(n) \\ z_{5x}(n) \end{bmatrix} = & - \begin{bmatrix} \frac{T_s^2}{m_3} \left(-\frac{2m_3}{T_s^2} + k_3 + k_4 \right) & -T_s^2 \frac{k_4}{m_3} & 0 \\ -T_s^2 \frac{k_4}{m_4} & \frac{T_s^2}{m_4} \left(-2\frac{m_4}{T_s^2} + k_4 + k_5 \right) & -T_s^2 \frac{k_5}{m_4} \\ 0 & -T_s^2 \frac{k_5}{m_5} & \frac{T_s^2}{m_5} \left(-\frac{2m_5}{T_s^2} + k_5 \right) \end{bmatrix} \begin{bmatrix} z_{3x}(n-1) \\ z_{4x}(n-1) \\ z_{5x}(n-1) \end{bmatrix} - \\ & - \begin{bmatrix} 1 & 0 & 0 \\ 0 & 1 & 0 \\ 0 & 0 & 1 \end{bmatrix} \begin{bmatrix} z_{3x}(n-2) \\ z_{4x}(n-2) \\ z_{5x}(n-2) \end{bmatrix} + \\ & + \begin{bmatrix} T_s^2 \frac{k_3}{m_3} \\ 0 \\ 0 \end{bmatrix} [z_{2x}(n-1)] \end{aligned} \quad (5)$$

Ten different scenarios are evaluated. In the first two scenarios, the structure remains healthy and in the rest of the scenarios, the structure is damaged. Regarding the damaged scenarios (see figure 2), the damage can be located inside or outside the substructure, but only one floor is damaged in each scenario. The damages consist in a reduction of the width of all vertical plates related to each floor. Two severity levels are analysed, a width reduction of a one third (figure 2a) and two thirds (figure 2b). These width modifications correspond to stiffness reduction of approximately 25% and 50%.

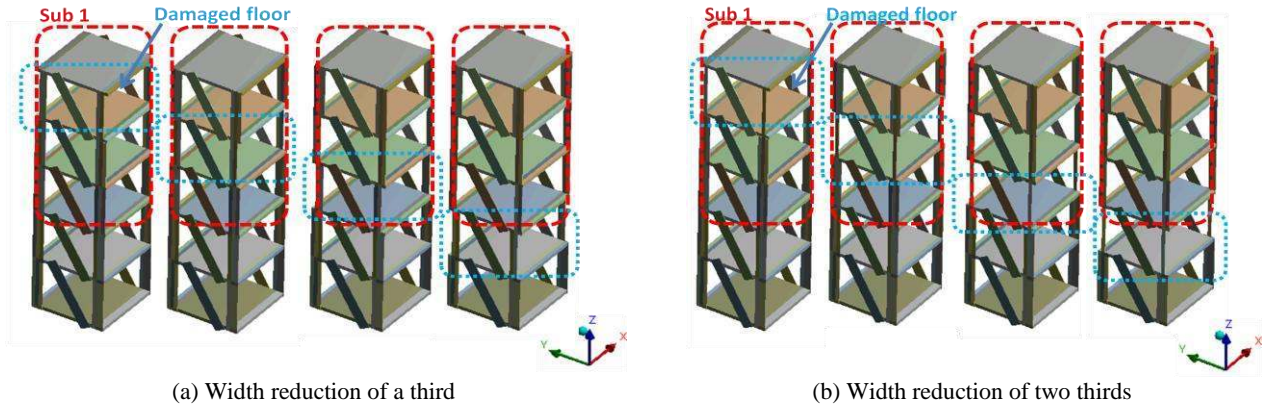


Figure 2: Evaluated damaged scenarios

The models are excited in the first floor and in the x direction by a Gaussian white noise force as it is shown in figure 1. Horizontal acceleration data ($\ddot{z}_{2x}, \ddot{z}_{3x}, \ddot{z}_{4x}$ and \ddot{z}_{5x}) is measured from the central node of each substructural slab with a data sampling frequency of 1000 Hz. The mentioned acceleration signals are integrated twice in order to obtain the corresponding horizontal displacements.

The substructural VARX model is estimated as in equation 5 for the initial scenario (reference) and also for the other ten scenarios that must be assessed. In all cases, the VARX models are estimated by the Multivariable Least-Square estimator (MLS) method using 3000 samples [14]. As it is explained in section 2, the condition of the substructure is evaluated analysing deviations between the new VARX models and the initial VARX model. The terms $A_{1(1,2)}$ and $A_{1(2,1)}$ are analysed to assess the condition of the fourth floor, the terms $A_{1(2,3)}$ and $A_{1(3,2)}$ for the fifth floor and the term $B_{1(1,1)}$ for the third floor.

Figure 3 presents the estimated stiffness modifications for each substructural floor in the ten analysed scenarios. Green, pink and blue bars represent the estimated stiffness reductions for the third, fourth and fifth floors respectively and the horizontal lines correspond to the real stiffness reduction caused in both severity levels.

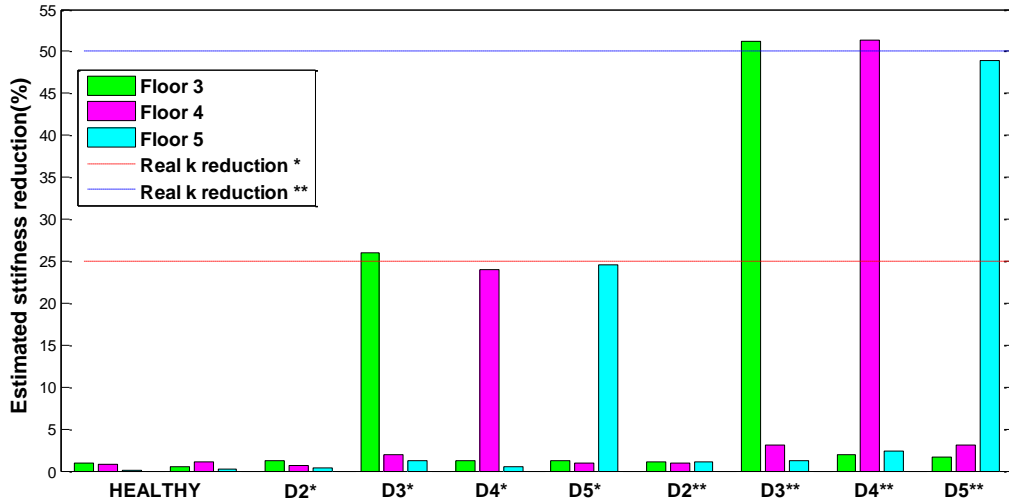


Figure 3: Estimated stiffness reduction for the analysed scenarios (*25%, **50%)

The results show that when certain damage is introduced within the substructure (floors 3, 4 or 5), the proposed method detects its presence, locates the damage in the correct floor and quantifies its severity. However, if the structure remains healthy or if the damaged elements are out of the substructure (floor 2), the estimated stiffness reduction is almost null.

In order to analyse the quality of the results, the root mean square (RMS) of the stiffness estimation error and the maximum stiffness estimation error are computed for each analysed scenario (see Table1). As three stiffness values must be estimated for each scenario (one per floor), the corresponding RMS value of the stiffness estimation error is calculated taken into account these three values. Furthermore, the maximum stiffness estimation error made in each scenario is given by the floor with the maximum estimation error.

Table 1: Stiffness estimation error for the analysed scenarios (*25%, **50%)

Scenario	Stiffness estimation error	
	RMS	MAX
Healthy	0.62%	1.03%
Damage in Floor 2 (*)	0.75%	1.21%
Damage in Floor 3 (*)	1.38%	1.13%
Damage in Floor 4 (*)	0.89%	1.89%
Damage in Floor 5 (*)	0.91%	3.06%
Damage in Floor 2 (**)	1.02%	1.15%
Damage in Floor 3 (**)	1.84%	2.42%
Damage in Floor 4 (**)	1.88%	1.28%
Damage in Floor 5 (**)	1.97%	3.12%
Global	1.29%	3.12%

Results show that the global RMS stiffness estimation error is 1.29% and the maximum stiffness estimation error is 3.12%.

4. EXPERIMENTAL EVALUATION

A five-story laboratory structure has been built in order to evaluate the proposed method. The structure is depicted in figure 4 and it has the same geometrical and material properties as the studied model in the previous section. The first five natural frequencies of the structure are 6.93 Hz, 20.97 Hz, 33.56 Hz, 43.07 Hz and 49.53 Hz.

As in section 3, a substructure formed by the upper three floors is selected for its monitoring. The horizontal acceleration data is measured within the substructure (\ddot{z}_{2x} , \ddot{z}_{3x} , \ddot{z}_{4x} and \ddot{z}_{5x}) with a data sampling frequency of 1652 Hz. This acceleration data is integrated twice to obtain the corresponding displacement data. As it is shown in figure 4, the structure is excited in the first floor and in the x direction by a Gaussian white noise force. The excitation force is generated by an electro mechanic shaker and it is applied by means of a stinger.

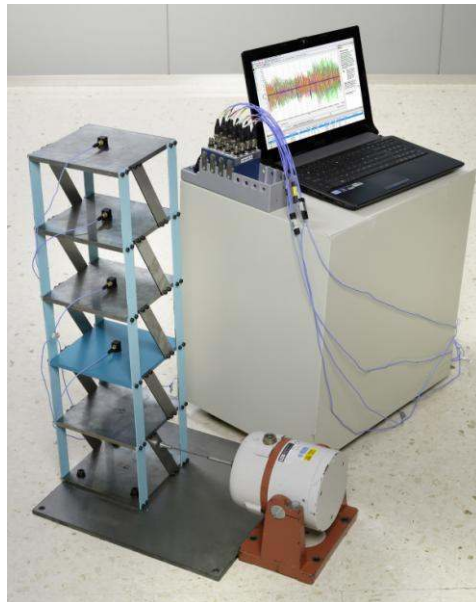


Figure 4: Experimental setup

Fourteen different scenarios are evaluated in this section. In the first two scenarios, the structure remains healthy and in the rest of the scenarios the structure is damaged, where damages are located within or out of the substructure. The damages are introduced replacing the original vertical plates by another narrower plates, which are two thirds narrower than the original ones. Within the same scenario the replaced plates are in the same floor, so only one floor is damaged in each scenario. Besides, three severity levels are evaluated, replacing one, two and four plates respectively. The mentioned severity levels correspond to a floor's stiffness reduction of approximately 12.5%, 25% and 50%.

The proposed SHM method is applied as in section 3, so a substructural VARX model is estimated for the initial healthy scenario and new VARX models are estimated for each new scenario. The VARX models are estimated by the Multivariable Least-Square estimator using 5000 samples. The condition of the substructure is evaluated analysing deviations in the matrices A_1 and B_1 .

Figure 5 presents the estimated stiffness modifications for the substructure in the fourteen analysed scenarios. Green, pink and blue bars represent the estimated stiffness reductions for the third, fourth and fifth floors respectively and the horizontal lines correspond to the real stiffness reduction caused in the three severity levels.

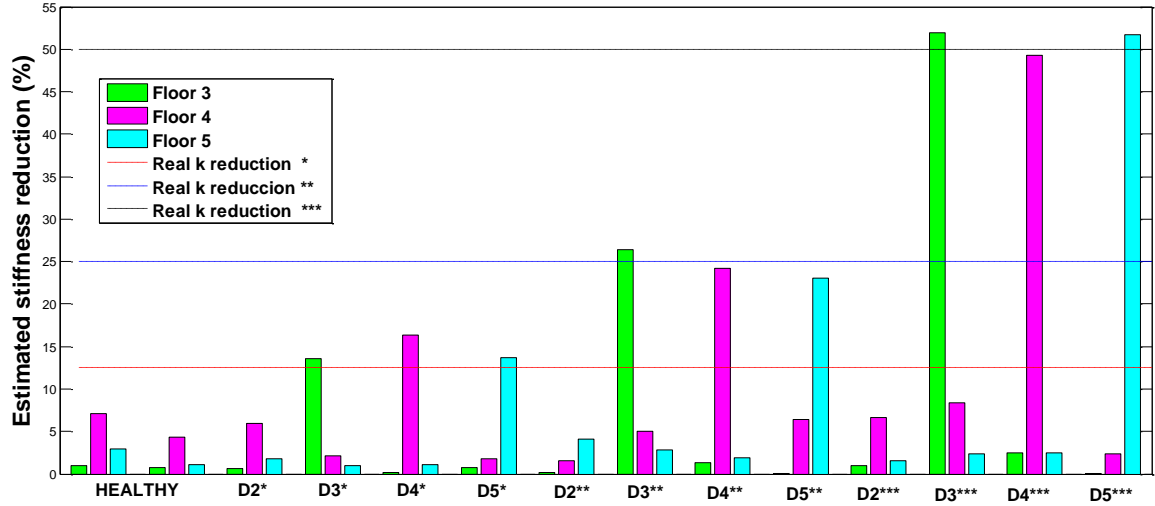


Figure 5: Estimated stiffness reduction for the analysed scenarios (*12.5%, **25%, ***50%)

The results show that when a certain damage is introduced within the substructure (floors 3, 4 or 5), the proposed method detects its presence, locates the mentioned damage in the correct floor and it quantifies the severity. However, if the structure remains healthy or if the damaged elements are out of the substructure (floor 2), the estimated stiffness reduction is much lower.

Table 2 shows the root mean square (RMS) of the stiffness estimation error and the maximum stiffness estimation error for the analysed scenarios. Both features are computed as in section 3.

Table 2: Stiffness estimation error for the analysed scenarios (*12.5%, **25%, ***50%)

Scenario	Stiffness estimation error	
	RMS	MAX
Healthy	2.84%	5.73%
Damage in Floor 2 (*)	2.77%	5.96%
Damage in Floor 3 (*)	1.97%	4.14%
Damage in Floor 4 (*)	3.05%	6.63%
Damage in Floor 5 (*)	1.41%	2.17%
Damage in Floor 2 (**)	3.07%	5.03%
Damage in Floor 3 (**)	4.22%	8.33%
Damage in Floor 4 (**)	1.69%	3.84%
Damage in Floor 5 (**)	1.36%	1.88%
Damage in Floor 2 (***)	1.89%	2.51%
Damage in Floor 3 (***)	1.24%	1.81%
Damage in Floor 4 (***)	2.79%	6.38%
Damage in Floor 5 (***)	1.37%	2.34%
Global	2.49%	8.33%

Results show that the global RMS stiffness estimation error is 2.49% and the maximum stiffness estimation error is 8.33%. Therefore, errors are 1.20% and 5.21% higher in the experimental verification than in the simulation ones.

5. CONCLUSIONS

This paper proposes a novel SHM method to detect, locate and quantify damages in structures. A substructure of interest is isolated by a substructuring method. Substructure's VARX model is estimated with the healthy data and it is taken as a reference. Substructural vibration data is measured again when the substructure must be evaluated and the corresponding VARX models are estimated. These new VARX models are compared to the reference in order to evaluate the condition of the substructure. Only vibration data is required to estimate the VARX models and it is not necessary to have a physics-based model.

The proposed method is validated by simulations and experimentally in a five-story laboratory structure. The results show that the method allows detecting, locating and quantifying damage within the substructure with a stiffness estimation error of 1.29% for the simulations and 2.49% for the experimental evaluation.

The proposed method is also suited for 3D lattice structures, where the number of element's connections increases. Our research group is already applying this method in 3D structures and the results will be published soon.

6. ACKNOWLEDGEMENT

This study is partially funded by the Ministry of Economy and Competitiveness of the Spanish Government (WINTURCON project, DPI2014-58427-C2-2-R). Any opinions, findings and conclusions expressed in this article are those of the authors and do not necessarily reflect the views of the funding agency.

REFERENCES

- [1] J. Ko and Y. Ni, "Technology developments in structural health monitoring of large-scale bridges," *Engineering structures*, vol. 27, pp. 1715-1725, 2005.
- [2] A. Mita, "Structural dynamics for health monitoring," Sankeisha Co., Ltd, Nagoya, vol. 114, 2003.
- [3] L. Jankowski, Lukasz and I. P. P. o. Techniki, *Dynamic load identification for structural health monitoring: Institute of Fundamental Technological Research Polish Academy of Sciences*, 2013.
- [4] S. W. Doebling, C. R. Farrar, M. B. Prime, and others, "A summary review of vibration-based damage identification methods," *Shock and vibration digest*, vol. 30, pp. 91-105, 1998.
- [5] J. Hou, L. Jankowski, Lukasz, and J. Ou, "Structural damage identification by adding virtual masses," *Structural and Multidisciplinary Optimization*, vol. 48, pp. 59-72, 2013.
- [6] C. G. Koh, L. M. See, and T. Balendra, "Estimation of structural parameters in time domain: a substructure approach," *Earthquake Engineering & Structural Dynamics*, vol. 20, pp. 787-801, 1991.
- [7] A. W. Oreta and T.a. Tanabe, "Element identification of member properties of framed structures," *Journal of Structural Engineering*, vol. 120, pp. 1961-1976, 1994.
- [8] Z. Xing and A. Mita, "A substructure approach to local damage detection of shear structure," *Structural Control and Health Monitoring*, vol. 19, pp. 309-318, 2012.

- [9]L. Mei, A. Mita, and Z. H. Xing, "Substructure damage detection method for shear structure using sub-time series and ARMAX," in *Key Engineering Materials*, 2013, pp. 149-159.
- [10]U. Ugalde, J. Anduaga, F. Martinez, and A. Iturrospe, "SHM method for damage localization based on substructuring and VARX models," arXiv preprint arXiv:1501.01905, 2015.
- [11]U. Ugalde, J. Anduaga, Martínez, F, and A. Iturrospe, "Novel SHM method to locate damages in substructures based on VARX models," in *Journal of Physics: Conference Series*, 2015, p. 012013.
- [12]L. B. Zhao, J. Y. Zhang, and Y. X. Zhao, "Taylor Series Numerical Method in Structural Dynamics," *Advanced Materials Research*, vol. 33, pp. 1213-1220, 2008.
- [13] P. J. Olver, "Introduction to partial differential equations", Springer, 2014.
- [14]H. Lutkepohl, "New introduction to multiple time series analysis," Springer, 2007.